THE JOURNAL OF BIOLOGICAL CHEMISTRY VOL. 288, NO. 43, pp. 31177–31191, October 25, 2013

RNF185 Is a Novel E3 Ligase of Endoplasmic Reticulum-associated Degradation (ERAD) That Targets Cystic Fibrosis Transmembrane Conductance Regulator (CFTR)*[S]

Received for publication, March 19, 2013, and in revised form, August 27, 2013 Published, JBC Papers in Press, September 9, 2013, DOI 10.1074/jbc.M113.470500

Elma El Khouri, Gwenaëlle Le Pavec, Michel B. Toledano, and Agnès Delaunay-Moisan[1]

From the Laboratoire Stress Oxydant et Cancers, Service de Biologie Intégrative et Génétique Moléculaire (SBiGeM), Institut de Biologie et de Technologies de Saclay (IBiTec-S), Commissariat à l'Energie Atomique-Saclay, 91191 Gif-sur-Yvette, Cedex, France

Background: RNF5 is an ERAD E3 ligase targeting CFTR to co-translational degradation, and RNF185 is an RNF5 homolog.
Results: RNF185 targets CFTR and CFTRΔF508 to co-translational degradation and synergizes with RNF5 to their post-translational degradation.
Conclusion: RNF185 and RNF5 act together as major ERAD E3 ligases of CFTR.
Significance: The RNF5/RNF185 module is a new potential therapeutic target for the treatment of cystic fibrosis.

In the endoplasmic reticulum (ER), misfolded or improperly assembled proteins are exported to the cytoplasm and degraded by the ubiquitin-proteasome pathway through a process called ER-associated degradation (ERAD). ER-associated E3 ligases, which coordinate substrate recognition, export, and proteasome targeting, are key components of ERAD. Cystic fibrosis transmembrane conductance regulator (CFTR) is one ERAD substrate targeted to co-translational degradation by the E3 ligase RNF5/RMA1. RNF185 is a RING domain-containing polypeptide homologous to RNF5. We show that RNF185 controls the stability of CFTR and of the CFTRΔF508 mutant in a RING- and proteasome-dependent manner but does not control that of other classical ERAD model substrates. Reciprocally, its silencing stabilizes CFTR proteins. Turnover analyses indicate that, as RNF5, RNF185 targets CFTR to co-translational degradation. Importantly, however, simultaneous depletion of RNF5 and RNF185 profoundly blocks CFTRΔF508 degradation not only during translation but also after synthesis is complete. Our data thus identify RNF185 and RNF5 as a novel E3 ligase module that is central to the control of CFTR degradation.

The endoplasmic reticulum (ER)[2] hosts a machinery called ERQC for ER quality control that is essential to prevent the secretion of improperly folded or assembled proteins (1–3). ERQC assists the production of functional proteins by promoting both the folding of nascent proteins through a cohort of chaperones, disulfide isomerases, and glycosylation enzymes and the degradation of terminally misfolded proteins through the so-called ER-associated degradation (ERAD) pathway (4). Both ERQC branches contribute to alleviate the folding stress imposed on the ER, thereby maintaining cell viability. When the burden of unfolded proteins overwhelms ER folding capacity, the unfolded protein response (UPR) is turned on to restore ER homeostasis.

ERAD encompasses a three-step process whereby misfolded proteins or unassembled subunits are first translocated from the ER lumen or ER membrane to the cytoplasm where they are finally targeted for degradation through the ubiquitin-proteasome pathway (5). Ubiquitination is a central process in ERAD as it tightly couples ERAD substrate recognition, efficient extraction, and retrotranslocation from the ER membrane to the cytoplasm and delivery to the proteasome. Ubiquitination involves the activation of the ubiquitin moiety by its loading on the E1-activating enzyme, the transfer of the ubiquitin moiety from the E1- to the E2-conjugating enzyme, and finally to the substrate by the coordinated action of the E2 and E3 enzymes (6). Two ER-associated E2 enzymes, Ubc6p and Ubc7p, and two ER membrane-embedded E3 ligases, Doa10p and Hrd1p, have been attributed to a major function in yeast ERAD (5). In mammals, functional homologs include E2s from the UBC6 and UBC7 family (7, 8), organized around an expanded number of E3 ligases (9, 10).

One of the best characterized E3 ligase-based complexes of ERAD is HRD (Hrd1-containing complex). This complex is conserved from yeast to mammals, and its core components are the E3 ligase Hrd1p (HRD1 in mammals) (11, 12) and the one pass ER transmembrane adaptor Hrd3p (SEL1L in mammals) (13). Although Hrd1p may directly participate in the recognition and ubiquitination of misfolded substrates (11, 14), Hrd3p both increases Hrd1p specificity and broadens its range of action (15). Indeed Hrd3p, by itself or through cooperation with the lectin chaperone Yos9p (OS-9 and XTP-3 in mammals) binds to and recruits substrates to the E3 ligase (13, 15, 16). In yeast, a functional HRD complex is also needed to support the interaction of Hrd1p with cdc48p/P97/VCP (17), the core subunit of the ATPase complex required for the dislocation of the substrate from the ER membrane and its delivery to the 26 S

* This work was supported by the Ligue Contre le Cancer, Vaincre la Mucoviscidose, the Fondation pour la Recherche Medicale, and Agence Nationale pour la Recherche (Project ERRed to M. B. T. and A. D. M.).
[S] This article contains supplemental Figs. 1–6 and Methods.
[1] To whom correspondence should be addressed: Laboratoire Stress Oxydant et Cancers, SBiGEM, IBiTec-S, CEA-Saclay, 91191 Gif-sur-Yvette Cedex France. E-mail: agnes.delaunay-moisan@cea.fr.
[2] The abbreviations used are: ER, endoplasmic reticulum; ERCQ, ER quality control; ALLN, *N*-acetyl-L-leucinyl-L-leucinyl-L-norleucinal-CHO; CHX, cycloheximide; ERAD, ER-associated degradation; MSD, membrane spanning domain; Q-PCR, quantitative PCR; UPR, unfolded protein response; RING, really interesting new gene; RM, Ring mutant.

proteasome (18–20). In mammals, the interaction of E3 ligases with p97 does not require their ligase activity (21), and the tight coupling between substrate ubiquitination and dislocation observed in yeast might thus be absent or uses alternate mechanisms. In both yeast and mammals, p97 also associates with proteins of the Derlin family, which are multipass transmembrane proteins, the function of which is still debated (17, 21, 22). Derlins interact with and are required for the degradation of select ERAD substrates (16, 23–27) as part of a distinct p97-containing complex bridged to the ligase (22). It was recently proposed that Derlins facilitate substrate extraction from the ER membrane, promoting their efficient delivery to the ERAD machinery (28). In yeast, Der1p is recruited to the HRD complex by Usa1p (Herp in mammals) (16), which otherwise regulates Hrd1p function through the regulation of its oligomerization, turnover, and activity (29–31).

In yeast, the two membrane-associated ERAD E3 ligases, Hrd1p and Doa10p, encompass most of the ERAD substrate repertoire (15, 16, 32, 33). Although Hrd1p is required for the ubiquitination of substrates bearing folding lesions in ER luminal and membrane domains, Doa10p is dedicated to those containing cytoplasmic lesions.

In mammals, an expanded number of ER-associated E3 ligases have been assigned to ERAD, the substrate specificity of which, if any, is not yet elucidated. These include two homologs of yeast Hrd1p, HRD1, and GP78, one homolog of Doa10p, TEB4, and enzymes that do not have homologs in yeast, RNF5/RMA1, RFP2, KF-1, and TRC8 (9, 33, 34). HRD1 and GP78 have multiple substrates, some of which are shared by these two ligases (35–39). Moreover, HRD1 might be preferentially in charge of ER soluble substrates (36, 38).

The RING finger-containing E3 ligase RNF5/RMA1 has recently gained interest because of its function in the degradation of the ERAD substrate CFTRΔF508, a mutant form of the cystic fibrosis transmembrane conductance regulator (CFTR), that is most frequently responsible for cystic fibrosis (27). CFTRΔF508 is targeted for ERAD at distinct folding stages, through the sequential action of the ligases RNF5/RMA1 and CHIP (27, 40–42). CHIP is a cytoplasmic U-box protein that is recruited on Hsc70-bound CFTR and targets it to ubiquitination and degradation after translation (27, 40–42). RNF5 rather senses CFTR folding defects during translation (27, 41) and may be recruited to CFTR lesions in part by the Hsc70-associated Hsp40 DnajB12 (43). RNF5 also associates with Derlin-1 to drive CFTR mutant degradation (27, 44). Current data support a model whereby RNF5 and GP78 collaborate to trigger CFTRΔF508 degradation, with RNF5 priming CFTRΔF508 by ubiquitination during translation and GP78 subsequently elongating the ubiquitin chain to promote efficient degradation (45).

We have here identified the RING finger-containing protein RNF185, a protein that is homologous by sequence to RNF5, as a novel ER-associated E3 ligase of ERAD. We show that RNF185 specifically targets CFTR and CFTRΔF508 to proteasomal degradation. As RNF5, RNF185 controls CFTR stability during translation, and combined inactivation of RNF185 and RNF5 leads to a dramatic stabilization of CFTRΔF508. Our data therefore uncover a functional overlap between these two ligases, which we further show takes place not only during but also after CFTR translation is complete. Overall, our data uncover a novel ERAD E3 ligase module important for the control of CFTR degradation in the ER.

EXPERIMENTAL PROCEDURES

Plasmids and Antibodies—Full-length human *RNF185* was cloned from HEK293 cells cDNA using Transcriptor High Fidelity cDNA synthesis kit (Roche Applied Science). It was then PCR-amplified using the primers GAAGATCTGCAAGCAAGGGGCCCTCGGCC and CCGCTCGAGTTAGGCAATCAGGAGCCAGAACATG and cloned into BamHI/XhoI sites of pcDNA3.1 FLAG expression vector. RNF185 deletion mutants (RNF185 ΔC, 1–176, and RNF185 ΔR, 94–192) were generated by PCR-based cloning of the corresponding fragments using, respectively, the following primers: CCGCTCGAGTTAGCGTGACAGGAACTGCTCGTC (down) for RNF185 ΔC GAAGATCTAGGGGCAGCACTGGGCAAC (up) for RNF185 ΔR. RNF185 RM (C39A, C42A) was generated by PCR-based mutagenesis using the following primers: CGAGGCCAACATCGCCTTGGACACAGCCAAGGATGCC (up) and CCAAGGCGATGTTGGCCTCGAAAGTGCTGTCCTGCC (down) and cloned along the same strategy used for the WT gene.

The pcDNA3.1 vectors expressing WT CFTR-HA and ΔF508 CFTR-HA, bearing an HA tag epitope in the C-terminal end of the proteins, were a generous gift from M. Benharouga. HA-CD3δ construct was a kind gift from A. Weissman (46). HA-TCRα was a kind gift from R. Kopito (47). α1-Antitrypsin-expressing vectors (NHK, Z mutants) were kindly provided by E. Chevet (University of Bordeaux). pEGFP-C1 (Clontech) was used as a control for transfection efficiency.

The following antibodies were purchased from commercial vendors: polyclonal anti-α1-antitrypsin (DakoCytomation); monoclonal MM13-4 anti-CFTR (N-terminal tail epitope) (Millipore); monoclonal clone 24-1 anti-CFTR (R & D Systems); polyclonal anti-Derlin-1 antibody (Sigma); monoclonal anti-Erlin2 (Sigma); monoclonal and polyclonal anti-FLAG antibodies (Sigma); monoclonal anti-GAPDH (Ambion); polyclonal anti-GFP (Abcam); monoclonal anti-HA (Covance); and monoclonal anti-ubiquitin (AssayDesign). Polyclonal anti-RNF5 was generated as described (48). Polyclonal anti-RNF185 was generated by injection of GST-RNF185 recombinant protein in rabbit and affinity purification of the resulting antibodies.

Cell Culture and Transfection—Human embryonic kidney (HEK) 293 or 293T cells were maintained in DMEM containing GlutaMAX (Invitrogen) supplemented with 10% fetal bovine serum in 5% CO_2 at 37 °C. Cells were transiently transfected using *Trans*IT-LT1 Transfection Reagent (Mirus) or using the calcium phosphate technique. HEK293 cells stably expressing CFTRΔF508 were generated by transfection with the expression vector pTracer (49) for CFTRΔF508 and selected with Zeocin (200 μg/ml).

Immunoprecipitation and Immunoblotting—For immunoblotting experiments, cells were washed with PBS and lysed on ice in buffer A containing 50 mM Tris-HCl, pH 8, 150 mM NaCl, 1% Triton X-100, 0.1% SDS, 1 mM EDTA, 0.5% deoxycholate, Protease Inhibitor Mixture tablets Complete (Roche Applied

Science), and 1 mM PMSF. Equal amount of proteins were loaded on SDS-PAGE after denaturation (5 min at 95 °C or 10 min at 42 °C for CFTR samples). Levels of endogenous RNF185 were monitored by immunoprecipitation using RNF185 polyclonal antibody in buffer A.

RNF185 partners were co-immunoprecipitated following lysis in IP buffer (50 mM Tris-HCl, pH 8, 150 mM NaCl, 0.5% Triton X-100, 1 mM EDTA, Protease Inhibitor Mixture tablets Complete (Roche Applied Science), and 1 mM PMSF). For CFTR/RNF185 co-immunoprecipitations, cell lysis was performed in a buffer containing 20 mM Hepes, pH 7, 150 mM NaCl, 1 mM EDTA, 1% Nonidet P-40 (buffer B). Immunoprecipitations were conducted with the indicated antibodies after a 15-min preclearance using 20 μl of Sepharose 4B beads. After extensive washing in lysis buffer, the samples were further processed for loading on SDS-PAGE.

Protein samples were separated on SDS-PAGE (6% acrylamide/bisacrylamide (40% 37.5:1) for CFTR samples or 14% for RNF185 samples) and transferred onto nitrocellulose membranes. After membrane blocking in 5% milk in PBS or in Odyssey blocking buffer (Li-Cor Biosciences), immunoblot analysis was performed using the indicated primary antibodies. Anti-mouse IgG or anti-rabbit IgG secondary antibodies labeled with fluorophores of different wavelengths were used to visualize specific protein signals by Infrared Imaging technology (Odyssey, Li-Cor).

For cycloheximide chase analysis, HEK293T cells were transfected with the indicated plasmids or siRNA, and 24 h or 48 h later, cells were treated with cycloheximide (Sigma, 100 μg/ml) for the indicated times.

Proteasome Inhibition—HEK293 cells were transfected with the indicated plasmids, and 24 h later treated with *N*-acetyl-L-leucinyl-L-leucinyl-L-norleucinal-CHO (ALLN, Calbiochem, 10 μg/ml) or the equivalent volume of DMSO for 12 h. Cells were lysed, and proteins extracted with buffer A. Soluble and insoluble fractions of protein lysates were analyzed by Western blot.

Pulse Labeling Analysis—After a 30-min incubation in a methionine/cysteine-free medium (Invitrogen), cells were incubated for the indicated times with a pulse-labeling medium containing EasyTag™ EXPRESS^{35}S Protein Labeling Mix (100 μCi/ml) (PerkinElmer Life Sciences). After the indicated labeling times, cells were washed with cold PBS and resuspended on ice in buffer B. After pre-clearing, the extracts were centrifuged, and 5× RIPA buffer (250 mM Tris-HCl, pH 7.5, 750 mM NaCl, 5% Triton X-100, 5% deoxycholate, 0.5% SDS) was added to the supernatants to reach a 1× final concentration. Immunoprecipitation was then performed using anti-HA antibody (transfected CFTR) or 24-1 anti-CFTR antibody (stable cell lines). After washing, immunoprecipitated material was denatured at 42 °C and loaded on a 6% SDS-PAGE. Fixed gels were then exposed on Biomax MR film (Sigma). When mentioned, cells were pretreated with ALLN or DMSO for 1 h in complete DMEM medium prior to starvation and then for 30 min in the starvation medium to achieve proteasome inhibition.

RNA Interference Analysis—HEK293T cells were transfected at a final concentration of 40 nM with siRNA oligonucleotides directed against RNF185 (5′-GAUAUUUGCCACAGCAUU-U-3′ or 5′-CUUCUGUUGGCCGUGUUUA-3′) or a nonspecific control (5′-UAGCAAUGACGAAUGCGUA-3′) using the calcium phosphate method. 24 h later, cells were then transfected with CFTR-HA WT or CFTRΔF508-HA plasmids. Trace amounts of EGFP-C1 plasmid were co-transfected with CFTR plasmids to control CFTR transfection levels. Cells were then collected 48 h after the initial siRNA transfection. *RNF185* silencing was controlled either by immunoprecipitation using RNF185 antibody followed by immunoblot or by RT-Q-PCR using RNF185-specific primers.

To perform *RNF5/RNF185* double knockdown, HEK293 cell lines stably expressing a control or a validated shRNA sequence targeting RNF5 (48) were generated. shRNA were expressed in the pSS-H1 vector (a gift from D. Billadeau, Mayo Clinic, Rochester MN) downstream of the RNA polymerase II-dependent H1 promoter.

Quantitative-PCR Analysis—Cells or tissues were collected and washed in PBS, and RNAs were extracted using Macherey-Nagel RNA extraction kit according to the manufacturer's instructions. 1 μg of RNAs was then used for cDNA synthesis using Moloney murine leukemia virus reverse transcriptase (Invitrogen) and hexaprimers (Roche Applied Science). Quantitative PCR was then performed using Bio-Rad iCycler IQ5 PCR Thermal Cycler. The PCR was performed using SYBR Green PCR MasterMix amplification reagent (Invitrogen) and transcript-specific primers. The housekeeping gene *GAPDH* was used as reference for cell experiments. *18 S* RNA and *PPIA1* genes were used as internal standards for expression analysis in tissues. The transcript-specific primers used are the following: human *RNF185* 5′-CTGTCACGCCTCTTCCTATTTGT-3′ (forward) and 5′-GCCCAGCATTAGGCAATCAG-3′ (reverse); mouse *RNF185* 5′-TCTTCTGTTGGCCGTGTTTACA-3′ (forward) and 5′-TTGCAGACTGGACACACTTGTC-3′ (reverse); *GAPDH* 5′-ATGGGGAAGGTGAAGGTCG-3′ (forward) and 5′-GGGGTCATTGATGGCAACAATA-3′ (reverse); *GRP78* 5′-CACAGTGGTGCCTACCAAGA-3′ (forward) and 5′-TGTCTTTTGTCAGGGGTCTTT-3′ (reverse); *RN18S* 5′-CGCCGCTAGAGGTGAAATTC-3′ (forward) and 5′-TTGGCAAATGCTTTCGCTC-3′ (reverse); *PPIA1* 5′-ATGGCAAATGCTGGACCAAA-3′ (forward) and 5′-GCCTTCTTTCACCTTCCCAAA-3′ (reverse).

For analysis of *RNF185* expression upon UPR induction, HEK293 cells were grown in a 6-well plate. 24 h later, cells were treated with tunicamycin (2 μg/ml) and harvested at the indicated times. The levels of RNF185 and GRP78, used as a control for UPR induction, were evaluated by Q-PCR and quantified using GAPDH as an internal standard.

In Vitro Ubiquitination Assay—Bacterially expressed GST-RNF5, GST-RNF185, and GST-RNF185 RING mutants were purified on FPLC using fast-flow GST columns (GE Healthcare). *In vitro* ubiquitination was performed according to the instructions provided with the ubiquitin conjugation initiation kit (Boston Biochem). Briefly, the assays were carried out at 37 °C in a 30-μl reaction mixture containing 0.5 M Hepes, pH 8.0, 250 nM E1 enzyme solution, 600 μM ubiquitin solution, 1 mM Mg-ATP solution, and 0.4 μM of separately provided E2 enzymes. Reactions were terminated by the addition of 20 μl of 5× SDS sample buffer, and proteins were separated by 10%

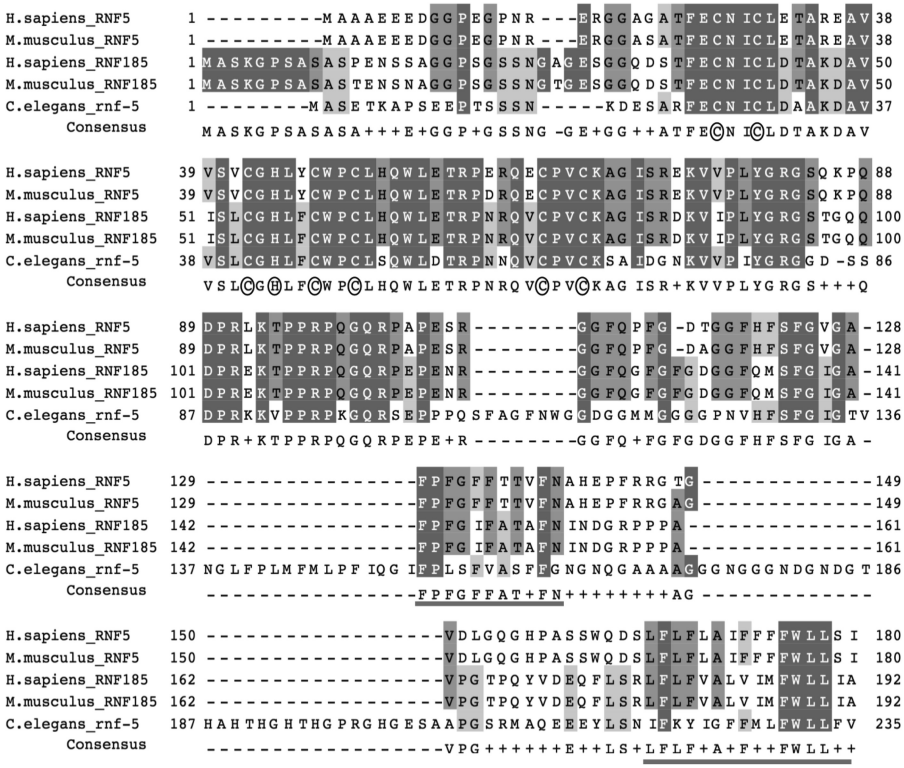

FIGURE 1. **RNF185 is an RNF5 homolog conserved in higher eukaryotes.** Amino acid sequence alignment is shown for human (GI, 45708382) and mouse (GI, 15928691) RNF185 with their human (GI, 5902054), mouse (GI, 9507059), and *Caenorhabditis elegans* RNF5 (GI, 3874385) homologs. The two C-terminal membrane domains are *underlined*. The seven cysteine residues and the histidine residue constitutive of the RING domain are *circled*.

SDS-PAGE and visualized by immunoblot using anti-GST and anti-ubiquitin antibodies.

Immunostaining—HEK293 cells were grown on coverslips and seeded on 24-well plates 24 h prior to TransIT transfection. Endoplasmic reticulum was visualized by co-transfecting ER-GFP (GFP KDEL) with the indicated plasmids. To visualize mitochondrial network, cells were treated for 45 min with 100 nM MitoTracker (Invitrogen) in DMSO prior to fixation. Cells were washed in PBS and fixed with 4% formaldehyde in PBS for 30 min. After three washes in PBS, cells were permeabilized using 0.5% Triton X-100 in PBS. For endogenous RNF185 staining, HEK293 cells were transfected with ER-GFP. 24 h after transfection, cells were washed in PBS and fixed with cold methanol for 4 min. Cells were then incubated with 3% BSA in PBS for 30 min. Cells were then incubated with the indicated antibodies (FLAG, 1:50,000; GFP, 1:20,000 in BSA 3% PBS). Image acquisition was done on a Zeiss LSM510 meta confocal microscope (Plan-Apochromat 63× 1.4-numerical aperture (NA1.4) objective). Images were further analyzed using ImageJ and Adobe Photoshop CS6 software.

RESULTS

RNF185 Is a Conserved Ubiquitous E3 Ligase of Higher Eukaryotes—By performing a BLAST analysis against the human RNF5 protein, we identified human RNF185, which exhibits more than 70% of sequence identity with RNF5. Apart from the RING domain, a high degree of sequence identity is found both in the two C-terminal transmembrane domains and in the central region (Fig. 1). By searching sequence databases, we identified homologs of RNF5 and RNF185 in several species. Drawing the phylogenic tree of the RNF family showed a clear partition of RNF5 and RNF185 into distinct taxonomic units, especially in mammals (supplemental Fig. S1). Such partition was less apparent in insects and plants, although several homologs were found in each organism. Interestingly, only one family member was found in nematodes, and no member could be found in *Saccharomyces cerevisiae*, although RNF5/RNF185 homologs exist in specific fungi and in amoebae. As shown by Q-PCR, *RNF185* is widely expressed in mouse tissues with high levels of expression in heart and testis (Fig. 2*A*).

To test the activity of RNF185 as a *bona fide* RING-dependent E3 ligase, we performed *in vitro* self-ubiquitination assays with GST-purified recombinant RNF185, in the presence of ubiquitin, ATP, E1, and different E2 enzymes. Auto-ubiquitination was monitored by Western blot using an anti-ubiquitin antibody (Fig. 2*B*). In the presence of UbcH5c, GST-RNF185 exhibited a potent self-ubiquitination activity that was comparable with that observed for RNF5. Self-ubiquitination, although much lower, could also be detected in the presence of UbcH6, but it was absent in the presence of UbcH7. We next tested the requirement of the RING domain for the ubiquitination activity of RNF185 by introducing two point mutations at cysteine 39 and 42 (RNF185 RM) or by truncating the entire RING domain (RNF185 ΔR) (see Fig. 2*C*). These mutants were both devoid of auto-ubiquitination activity (Fig. 2*D*), establishing that RNF185 has a RING-dependent E3 ligase activity.

RNF185 Localizes to the ER Membrane and Interacts with ERAD Components—Fluorescence microscopy was used to localize an N-terminal FLAG-tagged version of RNF185. In the

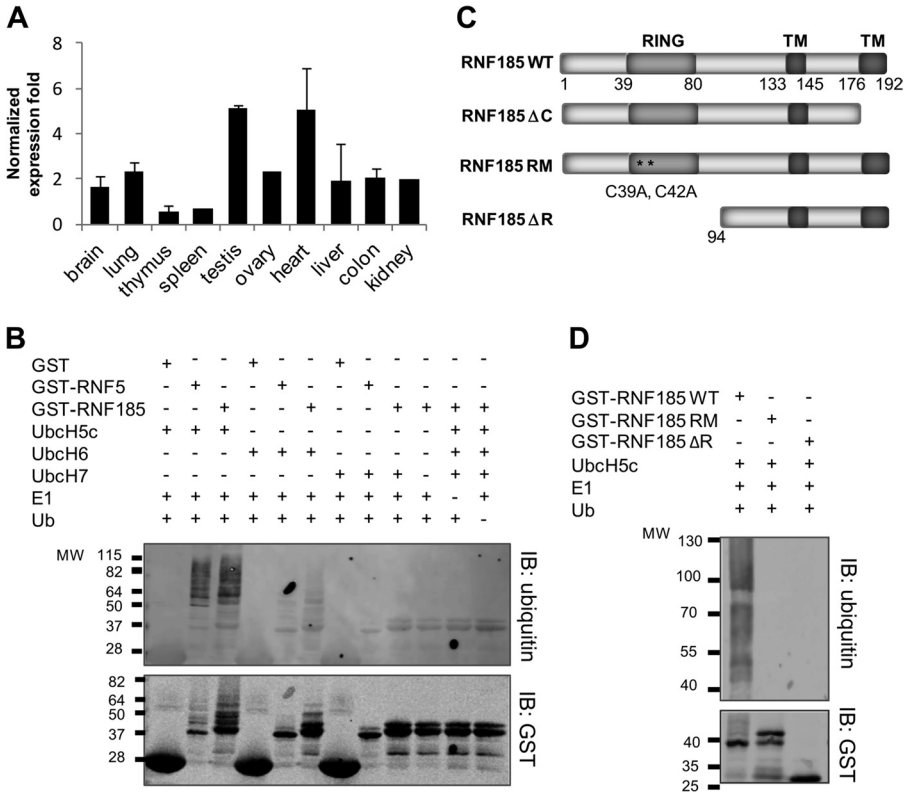

FIGURE 2. **RNF185 is a novel ubiquitously expressed E3 ligase.** *A,* expression of RNF185 in mouse tissues. Total RNAs were purified from WT mouse tissues and were retrotranscribed for quantitative-PCR analysis using *RNF185*-specific primers. *PPIA1* and *18 S RNA* were used as references. Analysis was carried out on RNA samples extracted from tissues of three different mice. *B,* RNF185 can auto-ubiquitinate. Purified GST, GST-RNF185, and GST-RNF5 were incubated at 37 °C in the presence of ATP, ubiquitin (*Ub*), E1, and three different E2 enzymes. The reaction was next subjected to immunoblotting (*IB*) with anti-GST or anti-ubiquitin antibodies. *C,* schematic representation of the RNF185 constructs used in this study. *RNF185 WT*, wild-type RNF185; *RNF185* Δ*C*, RNF185 with truncation of the most distal transmembrane domain; *RNF185 RM*, RNF185 with two punctal mutations in the RING domain; *RNF185* Δ*R*, RNF185 mutant with total deletion of the RING domain. *D,* RNF185 ubiquitin ligase activity is dependent on the RING domain. GST-RNF185 WT and its RING mutant counterparts were processed as in *B*.

HEK293 (Fig. 3*A*), HeLa, and RPE (supplemental Fig. S2, *A* and *B*) cell lines, RNF185 largely co-localized with the GFP-KDEL ER marker. Further in HEK293, endogenous RNF185 also localized to the ER, as shown using an antibody raised against RNF185 (Fig. 3*B* and supplemental Fig. S2*C*). A previous report indicated that RNF185 localizes to mitochondria and not to the ER (50), in discordance with our observations. We therefore compared the imaging-fluorescence signal of FLAG-tagged RNF185 with that of MitoTracker. Although we could not totally discount a mitochondrial localization (Fig. 3*C*), the ER localization of RNF185 appeared clearly predominant in our experimental conditions.

We next inspected the localization of FLAG-tagged mutants of RNF185 in HEK293 cells (Fig. 3, *A* and *C*). RNF185ΔC, a mutant with a truncation of the most distal transmembrane domain (amino acids 176–192) (Fig. 2*C*), did not localize to the ER, but instead it displayed a diffuse fluorescence pattern (Fig. 3, *A* and *C*), indicating that this domain is required for ER membrane targeting. In contrast, both RING mutants RNF185 RM and RNF185 ΔR essentially localized to the ER structure, indicating that the E3 ligase activity of RNF185 is not required for its localization.

Having shown that RNF185 is an E3 ligase localized in the ER, we next probed the interaction of its FLAG-tagged version with select ERAD components by FLAG immunoprecipitation in HEK293T cells. FLAG-RNF185 could efficiently pull down Derlin-1, as reported for FLAG-RNF5 (Fig. 4*A*). FLAG-RNF185, as well as FLAG-RNF5, also efficiently pulled down Erlin2 (Fig. 4*A*), a prohibitin-like scaffold protein of the ERAD that has been reported to target inositol triphosphate receptor (IP3R) (51). We next probed the RNF185 interaction with Ubc6 and Ubc7, which are the two ER membrane-associated E2 ligases of ERAD. FLAG-RNF185 efficiently pulled down both Ubc6e/UBE2J1 and UBE2J2 (Fig. 4*B*), but not Ubc7/UBE2G1 (data not shown), indicating a preferential association of RNF185 with the Ubc6 E2 ligase family.

As ERAD components are transcriptionally induced as part of the UPR (38, 52), we monitored RNF185 expression upon treatment with tunicamycin, a drug causing ER stress by blocking glycosylation. *RNF185* transcripts increased in response to tunicamycin, peaking at 12 h after the onset of treatment (Fig. 4*C*, *left panel*), a time course comparable with the one observed for the *bona fide* UPR target GRP78 (Fig. 4*C*, *right panel*). In summary, our data show that RNF185 is a RING domain-dependent E3 ligase of the ER that interacts with ERAD components and is transcriptionally induced during the UPR.

RNF185 Targets CFTR and CFTRΔF508 to ERAD—Our data strongly suggest a role of RNF185 in ERAD. To further substantiate this hypothesis, we checked whether modulating RNF185 cellular levels would affect the stability of ERAD model sub-

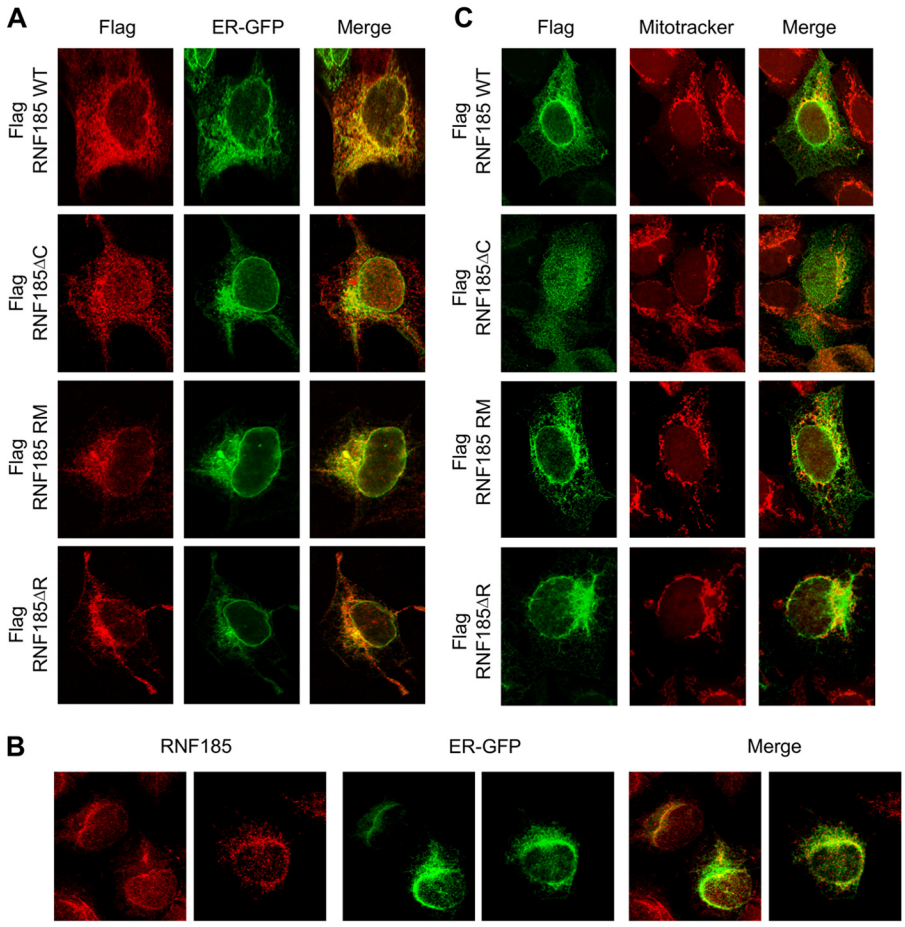

FIGURE 3. **RNF185 is an ER-localized E3 ligase.** *A,* co-immunolocalization of RNF185 WT and RNF185 mutants with ER marker. HEK293 cells were co-transfected with the different RNF185 constructs and a plasmid expressing an ER-localized GFP. Very low doses (0.1 μg of DNA per well of a 24-well plate) of plasmid were used to prevent overexpression bias. Cells were fixed 24 h after transfection and processed for immunostaining using FLAG antibody. *B,* immunolocalization of endogenous RNF185. 24 h after transfection with ER-GFP plasmids, cells were fixed and processed for immunostaining using homemade RNF185 polyclonal antibody. *C,* RNF185 co-localization with a mitochondrial marker. RNF185 constructs were transfected in HEK293 cells. 24 h after transfection, mitochondria were visualized by the addition of MitoTracker to the culture medium before processing the cells for immunostaining using FLAG antibody.

strates. CFTR and CFTRΔF508 are both targeted to ERAD, due to inefficient folding, which leads to the degradation of two-thirds of the former and 99% of the latter (53–55). CFTR migrates as two bands; the faster band represents the immature ER-localized B form, and the slower one represents the plasma membrane-localized mature C form (Fig. 5*A*, *upper panels*). CFTRΔF508 is only seen as the ER-retained immature B form. In cells overexpressing RNF185, the levels of both CFTR and CFTRΔF508 dramatically decreased, in proportion with the dose of RNF185 (Fig. 5*A*). Such an effect was dependent on RNF185 ubiquitin ligase activity, as it was not seen with the RING mutants RNF185 RM or RNF185 ΔR (Fig. 5*B*). At the highest dose of RNF185, intensity of the wild-type CFTR C form band was 5-fold lower (Fig. 5*A*, *lane 4*, 2 μg of DNA) than that of the control sample (Fig. 5*A*, *lane 1*). The RNF185-dependent decrease of the wild-type CFTR C form reflects an increased degradation of the ER-localized B form rather than a maturation defect, as suggested by the concerted change of immature and mature CFTR.

CFTRΔF508 levels also showed a 5-fold decrease upon RNF185 expression. Such a decrease was already seen at the lowest dose of RNF185 (Fig 5*A*), which suggests that CFTRΔF508 is more sensitive to RNF185-dependent degradation than CFTR.

We next evaluated the impact of RNF185 knockdown on the levels of CFTR proteins, using an *RNF185*-specific siRNA that potently extinguished *RNF185* expression up to 80% (Fig. 5*C* and supplemental Fig. S3). Under this condition, the intensity of the CFTR C form increased by 2-fold (202%). A minor increase of the intensity of the CFTR B form (121%) was also observed, again indicating that RNF185 affects CFTR turnover and not maturation (Fig. 5*C*). Knockdown of *RNF185* also resulted in a 2-fold increase in the intensity of the CFTRΔF508 B form, but it did not promote the appearance of the C form. The effect of the *RNF185* knockdown was also observed in a cell line stably expressing CFTRΔF508 (supplemental Fig. S3).

As a further indication of RNF185 and CFTR functional relationship, we checked their interaction by co-immunoprecipitation. Immunoprecipitation of either CFTR-HA or CFTRΔF508-HA could efficiently pulldown RNF185 or RNF185 RM in cells co-expressing these proteins but not in cells that did not (Fig. 5*D*, *upper panel*). Conversely, RNF185 RM immunoprecipitated CFTRΔF508-HA and the B form but not the C form of CFTR-HA (Fig. 5*D*, *lower panel*), validating

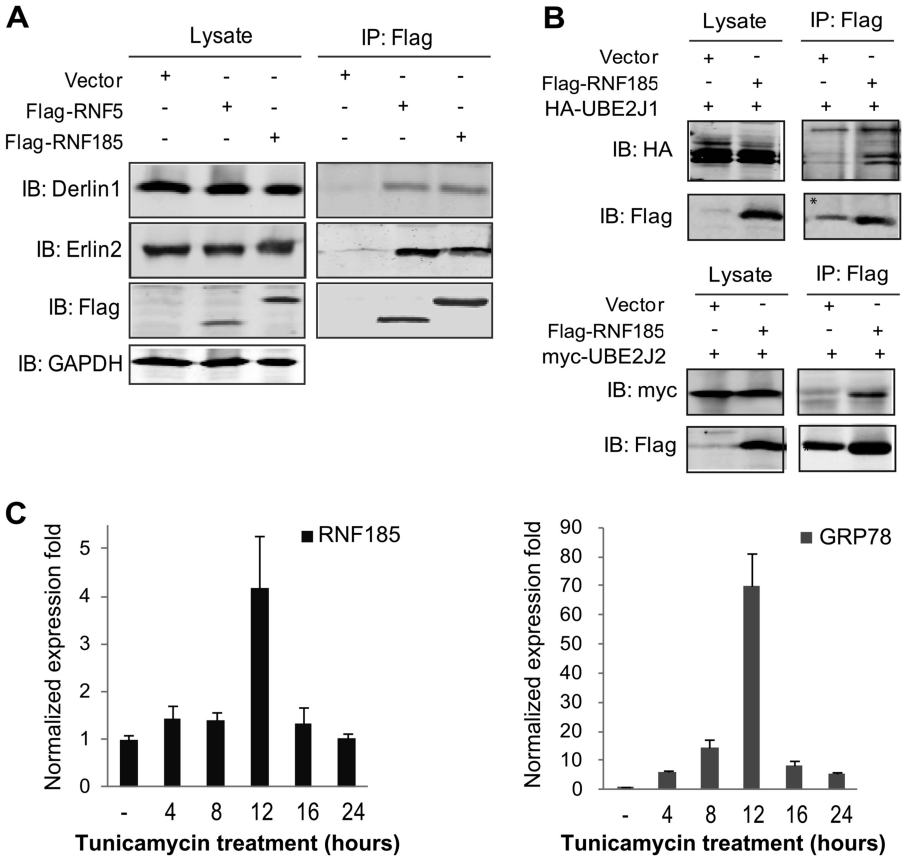

FIGURE 4. **RNF185 interacts with ERAD components and is induced by UPR.** *A,* RNF185 interacts with Derlin-1 and Erlin2. HEK293T cells were transfected with the control vector, FLAG-RNF185, or FLAG RNF5 (0.5 μg of plasmid per well of a 6-well plate). 24 h post-transfection, cells were lysed, and co-immunoprecipitation was performed using FLAG antibody. Immunoprecipitated (*IP*) proteins were loaded on reducing 14% SDS-PAGE and immunoblotted (*IB*) with antibodies against endogenous Derlin-1, endogenous Erlin2, or FLAG. *B,* RNF185 interacts with both enzymes of the Ubc6 family. HEK293T cells were transfected with the control vector or FLAG-RNF185 together with a plasmid expressing HA-UBE2J1 or myc-UBE2J2. Cells were then processed as in *A*. In this experiment, FLAG-RNF185 co-migrates with the antibody light chain as seen in the control lane (*). *C,* RNF185 expression is increased after tunicamycin treatment. HEK293 cells were treated with 2 μg/ml tunicamycin during the indicated times. Total RNAs were extracted and retrotranscribed. Q-PCR analysis was performed using *RNF185*-specific primers, and its expression levels were normalized to *GAPDH* levels (*left panel*). Results are shown as the mean of three independent experiments. Change in *GRP78* expression was used as a control for UPR induction by tunicamycin (*right panel*).

their functional interaction in the ER. Association with wild-type RNF185 was tested in the presence of the proteasome inhibitor MG132 to prevent RNF185-induced CFTR degradation (see below).

We also checked whether, in addition to CFTR, RNF185 could target other ERAD model substrates. TCRα and CD3δ are type I transmembrane proteins recognized as abnormal T cell receptor subunits when individually expressed and, as such, are degraded by ERAD (8, 56–59). The NHK and Z variants are folding-defective mutants of the ER luminal enzyme α1-antitrypsin. Although the NHK mutant is a *bona fide* ERAD substrate, the Z variant is cleared up by both the proteasomal and autophagic pathways (60–63). Overexpressing RNF185 did not affect the stability of any of these proteins (supplemental Fig. S4, *A* and *B*). Overexpressing E3 ligase RING mutants can cause dominant-negative effects by titration of their substrates away from E2-dependent ubiquitination. However, neither of the RNF185 RING mutants had an effect on the stability of the isolated TCR or mutant α1-antitrypsins (supplemental Fig. S4, *C* and *D*). Overall, these data indicate that RNF185 is a novel ER E3 ligase that regulates CFTR turnover.

RNF185 Affects CFTR and CFTRΔF508 Stability through the Ubiquitin-Proteasome System—To evaluate whether RNF185 affects CFTR turnover through proteasomal degradation, we monitored the effect of the proteasome inhibitor ALLN. Consistent with previous observations by Ward *et al.* (55), proteasome inhibition strongly stabilized WT and mutant CFTR, with preferential accumulation of the immature B form in both the detergent-soluble and detergent-insoluble fractions (Fig. 5*E*). ALLN also mitigated the RNF185-dependent decrease of both CFTR and CFTRΔF508 levels, an effect that was more pronounced for the latter. To detect CFTR-ubiquitin conjugates, we blocked protein deubiquitination by adding *N*-ethylmaleimide during the lysis of cells that were otherwise treated with proteasome inhibitors (supplemental Fig. S5*A*). In both ALLN- and MG132-treated cells, the amount of CFTR ubiquitin conjugates increased in the presence of RNF185, which indicates that RNF185 targets CFTR to ubiquitin-proteasome-dependent degradation.

As shown in Fig. 4*B*, RNF185 interacts with the E2 ligases Ubc6e/UBE2J1 and UBE2J2, the former of which is known to regulate CFTR turnover (7). We thus evaluated the role of these

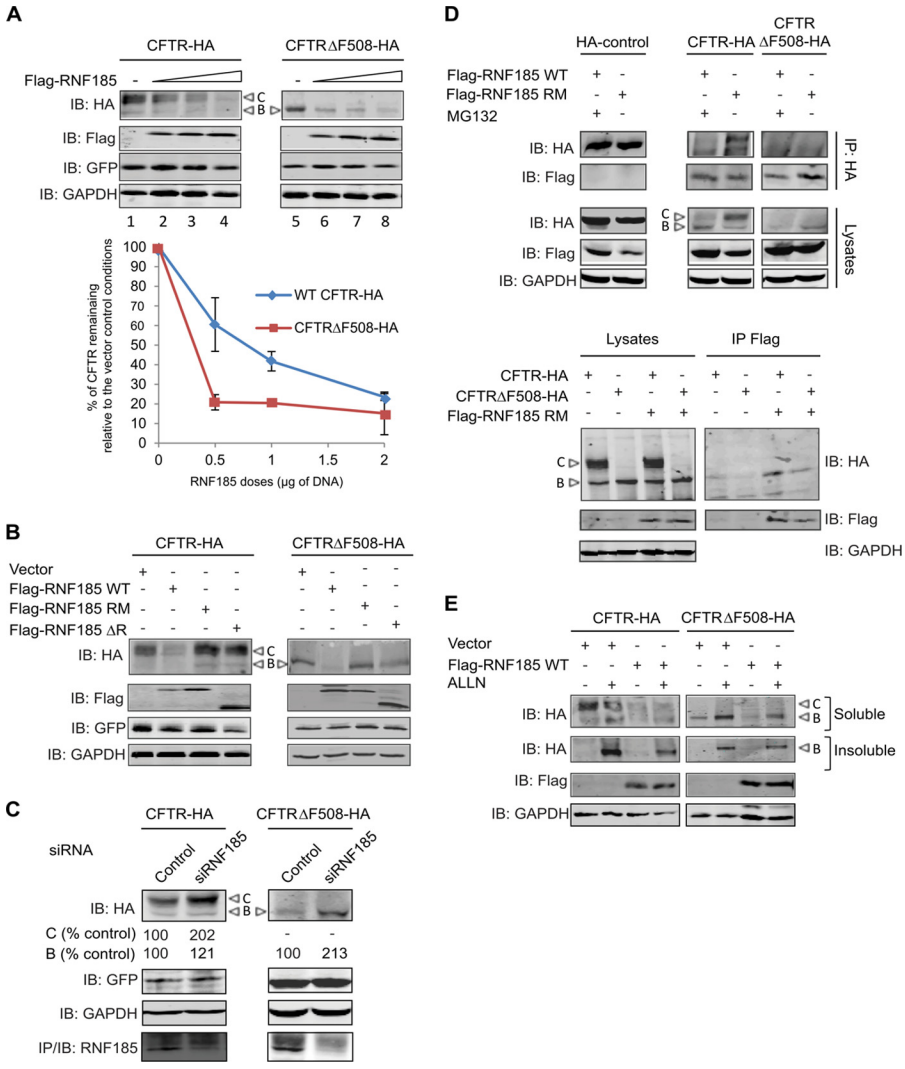

FIGURE 5. **RNF185 induces the ubiquitin-proteasome-dependent degradation of CFTR proteins.** *A,* RNF185 overexpression decreases the steady-state levels of WT CFTR and CFTRΔF508. Cells were co-transfected with control vector or increasing amounts of FLAG-RNF185 (0.5, 1, or 2 μg per well) and CFTR-HA or CFTRΔF508-HA. Low amount (0.1 μg per well) of a GFP-expressing plasmid was co-transfected in each condition, and the monitoring of GFP expression was used as a control for transfection efficiency. 24 h post-transfection, cells were lysed, and equal amounts of protein extracts were loaded on reducing SDS-PAGE for immunoblot (*IB*) with the indicated antibodies. GAPDH was used as a loading control. The core-glycosylated immature form and the mature-glycosylated form of CFTR are noted in *B* and *C*, respectively. Steady-state levels of CFTR and CFTRΔF508 were quantified using ImageJ software and were normalized to GAPDH and GFP levels. Results from three independent experiments have been plotted and are expressed as a percentage of the control (vector) condition. *B,* decrease in CFTR levels is dependent on RNF185 E3 ligase activity. Cells were co-transfected with control vector or vector expressing RNF185 WT, RNF185 RM, or RNF185 ΔR together with CFTR-HA or CFTRΔF508-HA. As in *A*, co-transfection with a GFP-expressing plasmid was used to monitor transfection efficiency. Cells were next processed as in *A*. *C, RNF185* knockdown increases CFTR levels. Cells were co-transfected with CFTR-HA or CFTRΔF508-HA together with a control or a *RNF185*-specific siRNA. 48 h later, the cells were processed as described in *A*. *RNF185* extinction was monitored after immunoprecipitation (*IP*) of the cellular extracts with anti-RNF185 antibody. Relative steady-state levels of CFTR proteins were quantified using ImageJ software. Results are expressed as a percentage of the control condition. *D,* RNF185 interacts with CFTR and CFTRΔF508. HEK293T cells were co-transfected with the indicated plasmids. HA-H3, a plasmid expressing HA-tagged histone H3, was used as a negative control for the immunoprecipitation (*upper panel*). Cells expressing WT RNF185 were treated with MG132 during 5 h before processing with the lysis. Co-immunoprecipitations were carried out with equal amounts of cell lysates using anti-HA antibody (*upper panel*) or anti-FLAG antibody (*lower panel*). The immunoprecipitates were next immunoblotted with the indicated antibodies. *E,* proteasome inhibition rescues RNF185-induced decrease in CFTR levels. HEK293 cells were co-transfected with the indicated plasmids and treated with ALLN or DMSO for 12 h, 24 h post-transfection. After cell lysis, the detergent-insoluble and -soluble fractions were subjected to immunoblot analysis with the indicated antibodies.

E2 ligases in RNF185-dependent CFTR degradation. Co-expressing RNF185 and Ubc6e/UBE2J1 decreased CFTRΔF508 levels in an additive manner that was not seen with the catalytically dead Ubc6eC91S (supplemental Fig. S5*B*, compare *lanes 2* and *3* with *lane 4*). These data suggest that these two enzymes cooperate in CFTR degradation. However, we could not observe a rescue of the RNF185-dependent degradation of CFTRΔF508 following Ubc6eC91S overexpression, an effect that would be expected on the basis of a transdominant negative effect of Ubc6eC91S. Therefore, either Ubc6eC91S does not behave as a transdominant negative mutant in these conditions or alternatively another E2 ligase cooperates with RNF185 to degrade CFTR. RNF185 also interacted with UBE2J2 (see Fig. 4*B*), yet simultaneously co-expressing both Ubc6 dominant-negative mutants did not prevent RNF185-dependent degradation of CFTR (data not shown). UbcH5 was previously shown to regulate CFTR degradation (42). After knocking down the expression of all three UbcH5 isotypes (a–c), we observed a partial rescue of RNF185-dependent decrease in CFTR levels (supplemental Fig. S5*C*). This suggests that the UbcH5 family

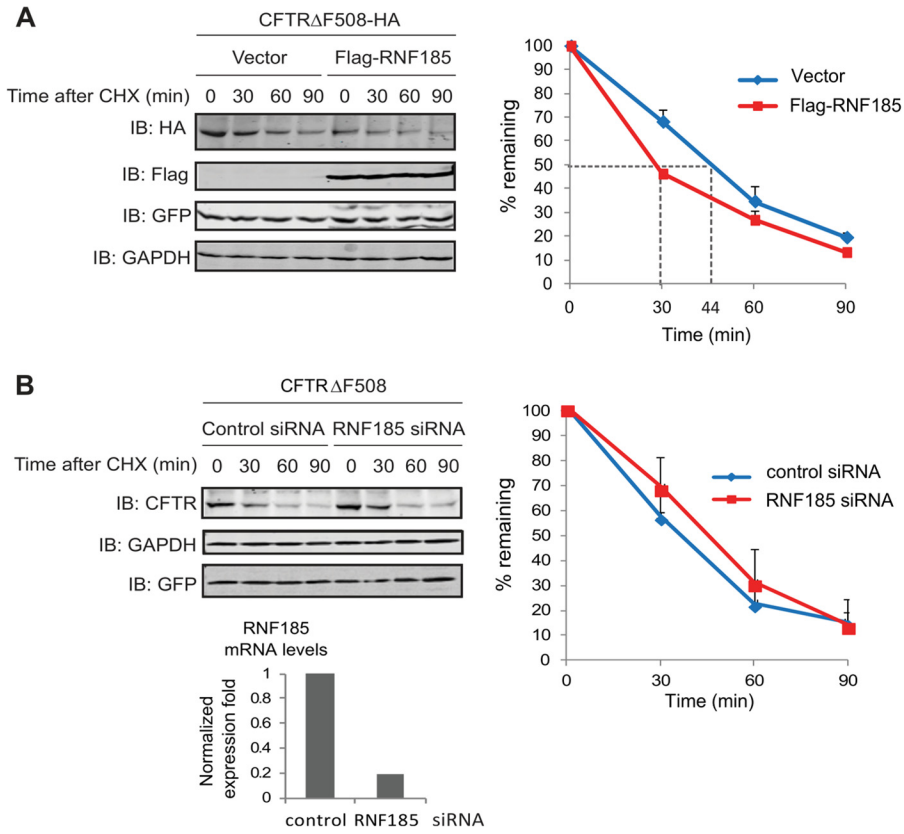

FIGURE 6. **Analysis of CFTRΔF508 degradation by cycloheximide chase.** *A,* CHX chase analysis of CFTRΔF508 upon RNF185 expression. HEK293T cells were co-transfected with CFTRΔF508-HA together with a control vector or vector expressing RNF185 WT. GFP-expressing plasmid was co-transfected as a marker for transfection efficiency. 24 h later, protein extracts were prepared at the indicated time points after cycloheximide treatment (100 μg/ml) and loaded onto reducing SDS-PAGE. Immunoblotting (*IB*) was performed with the indicated antibodies. Relative changes in the half-life of CFTRΔF508 were quantified from three different experiments using ImageJ software and normalized to GAPDH and GFP levels. The obtained values were plotted against time. *B,* CHX chase analysis of CFTRΔF508 upon *RNF185* knockdown. Cells stably expressing CFTRΔF508 were transfected with a control or an RNF185-directed siRNA. 48 h later, cells were treated with CHX and processed as in *A*. Down-regulation of *RNF185* expression was controlled by Q-PCR (*bottom panel in B*).

could also serve as E2 ligases for RNF185. In summary, these data indicate that RNF185 targets CFTR to degradation by the ubiquitin-proteasome system. However, they do not allow us to strictly identify the preferred RNF185-partner E2 ligase in this function, whether it is Ubc6e or UbcH5 or both.

RNF185 Affects CFTR Co-translational Degradation—We next sought to quantify the change in the rate of CFTRΔF508 degradation prompted by RNF185 overexpression through a measure of the CFTRΔF508 half-life, after inhibiting translation with cycloheximide (CHX) (Fig. 6). Upon RNF185 overexpression, the increased degradation of CFTRΔF508 was reflected by a decrease of its half-life from 44 to 29 min in the presence of RNF185 (Fig. 6*A*). Upon *RNF185* knockdown, however, despite an elevated level of CFTRΔF508 at the initial time point, the CFTRΔF508 half-life was not significantly altered (Fig. 6*B*). The CHX-based protocol only reports on the stability of fully translated CFTR protein, ignoring any co-translational degradation. To evaluate whether RNF185 could preferentially affect CFTRΔF508 stability during translation, we monitored the accumulation of metabolically labeled CFTRΔF508 after adding [^{35}S]Met/[^{35}S]Cys for a defined period of time (Fig. 7*A*). As expected, the amount of labeled CFTRΔF508 increased with time, but the overexpression of RNF185 decreased CFTRΔF508 labeling by up to 50% compared with the control condition. This decrease can be observed at all time points examined. The pulse labeling experiment measures the net balance between protein translation and degradation, the latter occurring after and possibly also during translation. To exclude an impact of RNF185 on CFTR translation efficiency, we repeated the pulse labeling experiment in the presence of the proteasome inhibitor ALLN. ALLN totally corrected the RNF185-dependent decrease of the amount of ^{35}S-labeled protein at all the time points tested (Fig. 7*A*), which indicates that RNF185 overexpression only affects CFTR degradation and not translation. The rate of post-translational degradation can be calculated from a fitted curve deduced from the values obtained in the CHX experiment (supplemental Fig. S6*A*), and this rate can then be used to predict the impact of post-translational degradation on the amount of accumulated ^{35}S-labeled CFTRΔF508 (see under "Appendix" and supplemental Fig. S6*B*). Such calculation predicts that the decrease in the amount of ^{35}S-labeled CFTR caused by RNF185 overexpression at 20 min would be 7% at best, if the degradation was exclusively post-translational, a decrease much lower than the 35–50% decrease observed in the pulse experiment (see "Appendix" and Fig. 7*B*). We thus conclude that upon overexpression, RNF185 targets CFTR proteins for ubiquitination and degradation both during and after protein synthesis.

We next performed the same experiment in conditions upon *RNF185* knockdown (Fig. 7*C*). Strikingly, the amount of accu-

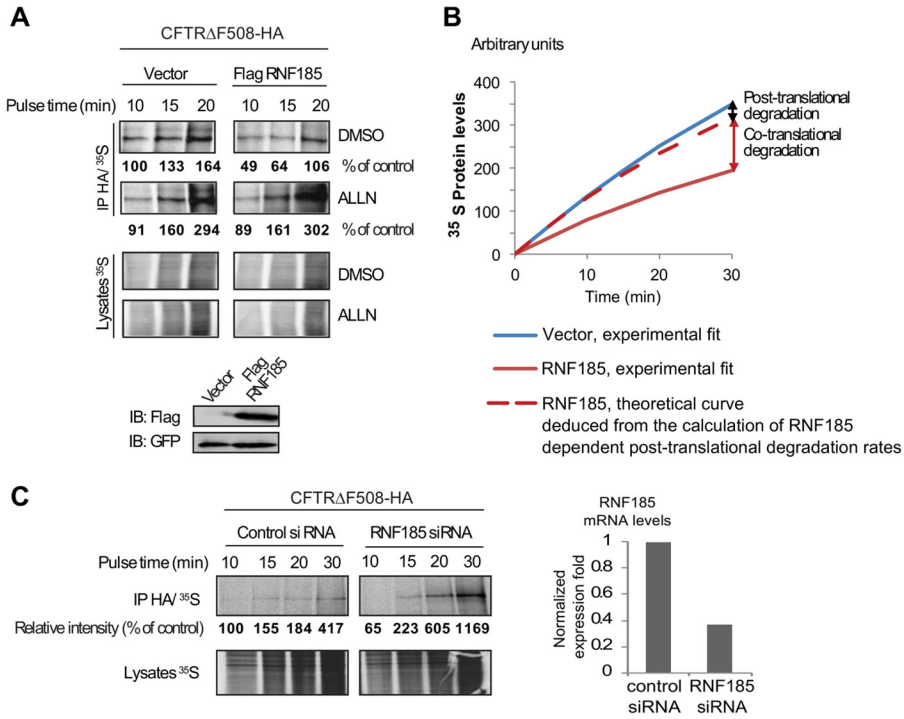

FIGURE 7. **RNF185 targets CFTRΔF508 to co-translational degradation.** *A,* measure of CFTRΔF508 labeling rates upon RNF185 overexpression. Cells were co-transfected with CFTRΔF508-HA together with RNF185 or the corresponding control vector. 24 h later, the cells were labeled with [^{35}S]Met/Cys radiolabeling mixture, and the synthesis of ^{35}S-labeled CFTRΔF508 protein was monitored over time by immunoprecipitating equal amounts of the labeled extracts with anti-HA antibody. ALLN or DMSO was added in the medium 90 min before labeling. Consistency of ^{35}S labeling between samples was controlled by loading the supernatants of the corresponding immunoprecipitation (*IP*) (depicted as *lysates* ^{35}*S*). Quantification of the experiment was performed using ImageJ software, and the intensity of labeled CFTR was normalized to the total amount of radioactivity initially present in the corresponding lysate. Results are expressed as a percentage of the vector condition quantified at 10 min in DMSO. RNF185 expression was confirmed by SDS-PAGE analysis (*lower panel*). *IB*, immunoblot. *B,* comparison of the experimental fitted curves (*solid lines*), accounting for the observed accumulation of ^{35}S-labeled CFTRΔF508 over time in the absence (*blue line*) and presence (*red line*) of RNF185, with the theoretical curve (*dashed red line*) predicting the accumulation of ^{35}S-labeled CFTRΔF508 if RNF185 only impacted the CFTR post-translational degradation rate. The experimental fitted curves were obtained as described under the "Appendix" and in supplemental Fig. S6. The theoretical RNF185 curve was obtained by setting equal rates of synthesis in the presence or absence of RNF185. *C,* measure of CFTRΔF508 labeling rates upon *RNF185* knockdown. Cells stably expressing CFTRΔF508 were transfected using control or *RNF185*-directed siRNA. 48 h after transfection, the cells were labeled and processed as in *A*. Efficiency of *RNF185* knockdown was controlled by Q-PCR analysis (*right panel*).

mulated ^{35}S-labeled CFTRΔF508 was at least twice the control condition. As *RNF185* knockdown did not affect the rate of CFTR post-translational turnover (see Fig. 6*B*), these data again point to a preferential effect of RNF185 on CFTR stability during synthesis.

RNF5 and RNF185 Have a Redundant Function on the Control of CFTR Stability—The control of CFTR co-translational degradation has previously been attributed to RNF5 (27). We therefore compared the impact of RNF5 and RNF185 knockdown on CFTR turnover. Initial assays using *RNF5*-specific siRNA did not produce any significant stabilization of CFTRΔF508. However, HEK293 cells stably expressing an *RNF5*-directed shRNA sequence succeeded, as it caused a 3-fold increase in CFTRΔF508 steady-state levels (Fig. 8), compared with the 2-fold increase observed upon *RNF185* knockdown (see Figs. 5*C* and 8). As already shown above for *RNF185*, the effect of each single knockdown mainly reflected an E3 ligase-dependent co-translational regulation of CFTR stability, as each did not significantly impact CFTRΔF508 turnover rate after CHX addition (Figs. 6 and 8). We next monitored the impact of knocking down *RNF5* and *RNF185* simultaneously. Strikingly, the combined depletion of both ligases led to a drastic stabilization of CFTRΔF508. This was reflected by a 4.5-fold increase in CFTRΔF508 steady-state levels and also by a net decrease of CFTR turnover rates after CHX addition. Importantly, the pool of stabilized CFTRΔF508 was only found in the Triton-soluble fraction (data not shown), indicating that stabilized CFTR proteins do not form aggregates and should be accumulating in a foldable state.

These data strongly suggest that RNF5 and RNF185 are functionally redundant in the control of CFTR stability. Moreover, they reveal a new overlapping function for these enzymes in the post-translational control of CFTR stability.

DISCUSSION

We have herein characterized RNF185 as a novel RING E3 ligase of the mammalian ERAD machinery. We have shown that, as demonstrated for many other ERAD components, RNF185 is an ER-associated E3 ligase whose expression is induced upon ER stress. As such, RNF185 affects the stability of the ERAD substrates CFTR and CFTRΔF508 in a RING domain- and ubiquitin-proteasome-dependent fashion but not that of the other ERAD model substrates TCRα, CD3δ, and α1-antitrypsin. Whether RNF185 indeed is specific for CFTR proteins remains to be tested by the use of a broader range of ERAD substrates, including other multipass membrane proteins. Our data indicate that RNF185 can sense CFTR folding defects while CFTR is being synthesized, a function previously

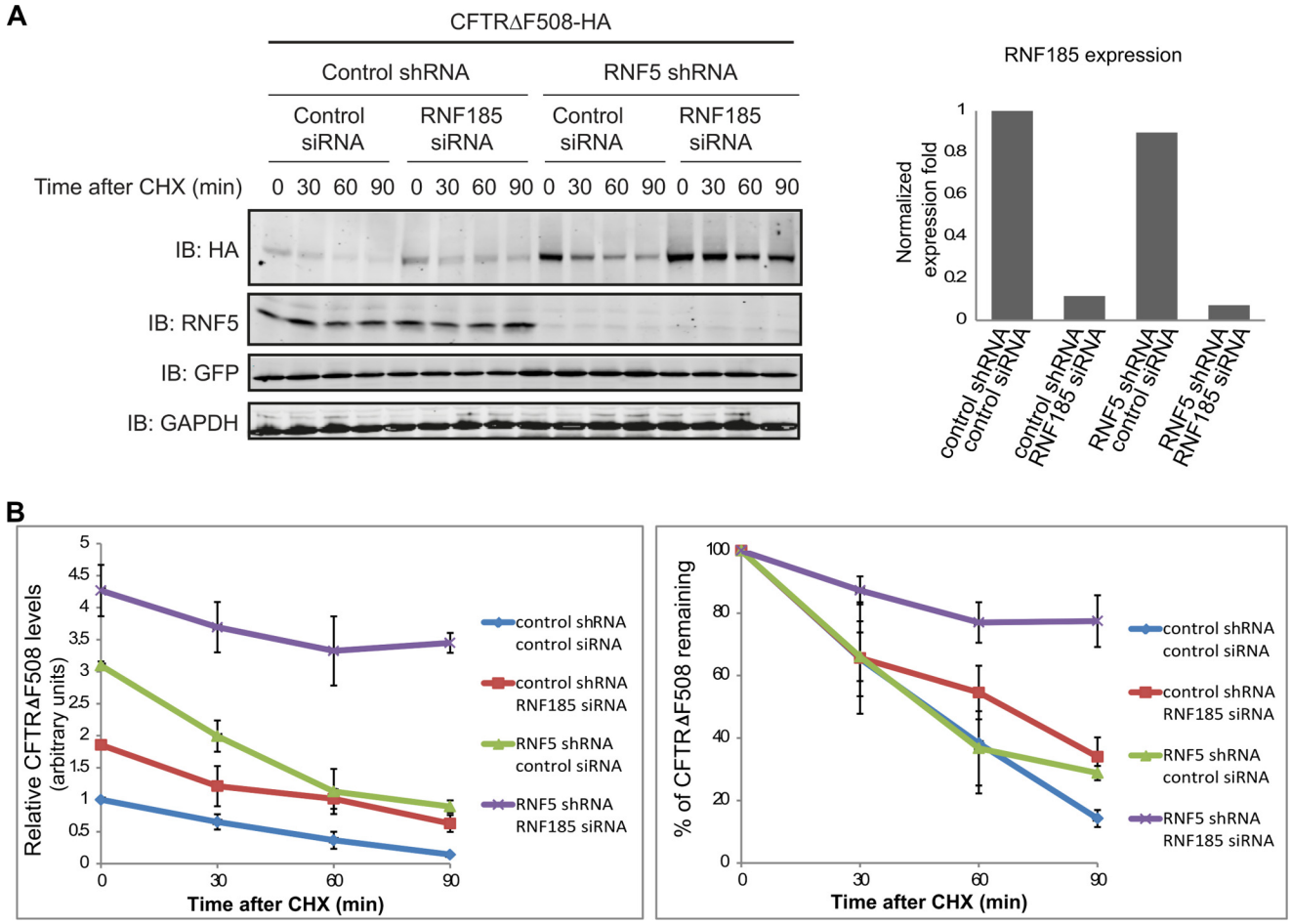

FIGURE 8. **Combined depletion of RNF185 and RNF5 synergistically blocks CFTRΔF508 degradation.** *A,* analysis of CFTRΔF508 turnover upon combined *RNF185* and *RNF5* knockdown. HEK293 cells stably expressing a control shRNA or an shRNA sequence targeting *RNF5* were co-transfected with CFTRΔF508-HA together with a control siRNA or a siRNA sequence targeting *RNF185*. 48 h later, the cells were treated with CHX for the indicated times and processed as in Fig. 6*A*. Immunoblotting (*IB*) following SDS-PAGE was performed using the indicated antibodies. Down-regulation of *RNF185* expression was controlled by Q-PCR (*right panel*). *B,* relative changes in the half-life of CFTRΔF508 were quantified from three independent experiments using ImageJ software and normalized to GAPDH and GFP levels. The obtained values were plotted against time. *Left panel* is depicting relative values normalized to the control condition (control shRNA, control siRNA), where initial CFTR ΔF508 levels in this condition have been artificially normalized to 1. The *right panel* is depicting CFTRΔF508 intrinsic half-life after translation block, the initial time point for each condition being set at 100%.

attributed to RNF5. Simultaneous depletion of RNF185 and RNF5 indeed unraveled their functional redundancy in controlling CFTR degradation. Importantly, our data now indicate that the combined depletion of RNF5 and RNF185 blocked CFTR turnover not only during translation but also after CFTR synthesis has been completed. We thereby uncovered a new redundant function of these E3 ligases in controlling the stability of full-length CFTR proteins.

RNF185 Functions in CFTR ERAD—Interaction data suggest that RNF185 belongs to a functional complex that includes the general ERAD components Erlin2, Derlin1, and E2 ligase Ubc6e, of which the latter two have previously been shown to contribute to CFTR turnover. Our data also suggest that Ubc6e might cooperate with RNF185 in targeting CFTR to degradation. However, our data also show that this functional interaction is not exclusive and that E2s from the UbcH5 family can also cooperate with RNF185, which is in agreement with the identification of the E2 enzymes as RNF185 interacting partners, along with other E2 enzymes (64). The effect of UbcH5 knockdown on the RNF185-stimulated degradation of CFTR is, however, hard to interpret as UbcH5 depletion also impacts CHIP-dependent CFTR degradation (42). Thus, which of the two E2 enzymes is the *bona fide* RNF185 partner in CFTR degradation or whether both types of E2 contribute to this function cannot be strictly established from our data. In fact, this situation is reminiscent of the one for RNF5, for which its co-expression with Ubc6e had an additive effect on CFTR stability, although its co-expression with mutant Ubc6e failed to restore CFTR levels above the ones monitored in cells expressing RNF5 alone (27). Moreover, UbcH5a mutant expression can partially prevent RNF5-stimulated CFTR degradation, suggesting RNF5 can also team up with enzymes of the UbcH5 family. It is thus possible that both RNF185 and RNF5 use alternative E2s to stimulate CFTR degradation.

RNF185 Can Target CFTR and CFTRΔF508 for Degradation during Translation—CFTR folding is a complex process, which involves cooperativity between protein domains and occurs both during and after translation (65). Not surprisingly, CFTR quality control is exerted both during and after translation, as indicated by studies on the turnover rates of CFTR mutant proteins (27) and CFTR ubiquitination during translation (14, 55). The latter observation thus suggests the existence of E3 ligases

that operate during CFTR synthesis. A role for RNF185 as one of these ligases is strongly suggested by our pulse labeling and turnover experiments. Upon ^{35}S pulse labeling (see Fig. 7, *A* and *B*), RNF185 overexpression caused a 50% decrease in the amount of ^{35}S incorporated into CFTRΔF508 relative to the control, which was much greater than the 7% theoretical decrease in the case of exclusive post-translational degradation. The involvement of RNF185 in CFTR co-translational quality control is further supported by our knockdown experiments, indicating a lack of post-translational stabilization of CFTRΔF508 after CHX-dependent translation arrest (Fig. 6*B*) and a significant increase in the amount of CFTR synthesized upon RNF185 extinction (Fig. 7*B*). That RNF185 affects CFTR co-translational degradation is also supported by our observation that RNF185 associates with Derlin-1, a protein suggested to promote CFTR ERAD early during synthesis by virtue of its interaction with CFTR N-terminal domains (25).

A Partly Redundant Function for RNF185 and RNF5—Among the two E3 ligases previously shown to affect CFTR stability in the ER (27, 40, 42), RNF5 and CHIP, a preferential role in the co-translational sensing of CFTR folding defects was attributed to RNF5. Our data now strongly indicate that RNF185 and RNF5 cooperate to target CFTRΔF508 to degradation not only during but also after its synthesis. Indeed, we show that simultaneous inactivation of these two E3 enzymes leads to a greater increase of CFTR levels compared with the one achieved upon their single inactivation. Simultaneous inactivation of these two E3 enzymes also dramatically decreased CFTRΔF508 post-translational turnover rates, as measured upon translation inhibition. Such an effect could only be uncovered once both E3 ligases have been depleted. Mechanistically, RNF5 and RNF185 redundancy could be assigned to both ligases sensing similar CFTR folding defects. Therefore, as depletion of either ligase alone stabilizes CFTR, strict redundancy would imply that the activity of each is limiting, at least in our experimental conditions. Conversely, RNF5 and RNF185 might sense different folding defects. In this case, their simultaneous depletion would be additive compared with their single knockdown. Such effect is only observed when measuring CFTR co-translational degradation rates, although RNF5 and RNF185 appear fully redundant after the synthesis of the full-length CFTR. We therefore favor an hypothesis where RNF5 and RNF185 might sense different folding defects during CFTR synthesis and similar ones after its synthesis had been completed. This would explain why RNF185 and RNF5 overexpression both decrease CFTR post-synthetic turnover rates, although their single knockdown does not. Analysis of mutated and truncated forms of CFTR was used to pinpoint the CFTR folding lesions preferentially sensed by RNF5. RNF5 was proposed to sense a defect in both the cooperative folding of the N-terminal regions occurring after synthesis of the R domain and the association of the two MSD domains (27, 41). Our preliminary data also indicate that RNF185 preferentially affects the turnover of CFTR proteins truncated after the R domain,[3] suggesting that as for RNF5 the synthesis of MSD2 and NBD2 C-terminal domains is not strictly required for RNF185-dependent quality control. Further experiments are needed to discriminate the mechanisms of RNF5- and RNF185-dependent checkpoints. Moreover, the relative impact of knocking down either ligase might depend on a given cell type and/or physiological condition.

The high degree of post-synthetic stabilization achieved by the double *RNF5/RNF185* knockdown also questions the function of CHIP. In the ER, CHIP was proposed to preferentially act post-translationally, targeting CFTRΔF508 to degradation once the second transmembrane domain (MSD2) of CFTR had been synthesized (27). CHIP overexpression was shown to affect CFTR post-synthetic degradation rates (42). However, knockdown-based experiments supporting this model are currently lacking. Experiments are now underway to investigate the relative importance of CHIP compared with RNF5 and RNF185 in stimulating CFTR post-translational degradation in the ER.

Could Other RNF185 and RNF5 Functions Explain the Need for Their Functional Redundancy in ERAD?—Functional redundancy between RNF5 and RNF185 could be rationalized by the need of a backup for RNF5 ERAD function, when this protein is diverted to competing processes such as the regulation of JAMP activity and the recruitment of the proteasome to the ER membranes (66), RNF5 mitochondrial recruitment and function in innate immunity signaling (67, 68), or its recently described role in the regulation of mitochondrial fission (69) and autophagy (70). RNF185 also appears to carry out distinct cellular functions, including control of Wnt signaling-induced paxillin degradation and regulation of mitophagy (see below). As such, it will be critical to assess the relative importance of the RNF module in CFTR degradation using more physiological settings, including bronchial epithelial cells and CF mouse models. It is important to emphasize that both RNF5 and RNF185 do not belong to the group of the archetypal ERAD multipass Hrd1p and Doa10p E3 ligases that are conserved from yeast to mammals. As such, they may be more likely to have versatile cellular or organismal functions in addition to the one we have described here in ERAD.

Other RNF185 Functions—A homolog of mammalian RNF185 was previously characterized in *Xenopus laevis* as a protein affecting the stability of the cytoplasmic substrate paxillin by direct recruitment of the proteasome (71). Wnt signaling-induced paxillin ubiquitination in the mesoderm was shown to lead to RNF185-dependent substrate degradation. However, this process might be indirect as paxillin ubiquitination was not shown to be operated by RNF185. This RNF185 function therefore differs from that described herein in ERAD.

RNF185 was also recently described as a positive regulator of mitophagy, a function that requires its ubiquitin ligase activity (50). According to this study, ubiquitination of the Bcl-2 family member BNIP1 by RNF185 increases autophagosome formation by promoting p62 recruitment to mitochondria. Although we did not directly address this question, our data could not demonstrate an effect of RNF185 overexpression on the Z mutant of α1-antitrypsin, the degradation of which is partly autophagic (60). It thus seems unlikely that RNF185 has broad effects on autophagy. Instead, such a function of RNF185 in

[3] E. El Khouri, G. Le Pavec, M. B. Toledano, and A. Delaunay-Moisan, unpublished data.

autophagy might be limited to its mitochondrial localization. Interestingly, the data by Tang and co-workers (50) and ours suggest that RNF185 could provide a new link between ERAD and autophagy, as was recently shown for RNF5 (70). Identification of physiological conditions potentially regulating RNF185 localization or function in autophagy will thus be of interest to further unravel intertwined functions of RNF185 and evaluate their consequences on CFTR turnover.

Conclusion—We have identified RNF185 as a new E3 ligase that drives CFTR degradation in the ER, a function that appears redundant with RNF5. These data expand the repertoire of mammalian E3 ligases that operate in ERAD. Importantly, they provide key information for setting up strategies to efficiently block CFTR degradation in the ER and to increase the pool of foldable CFTR, potentially operational for maturation and plasma membrane targeting. Evaluating the impact of CFTR correctors, especially chemical chaperones, on the maturation of this stabilized pool will be critical to assess the therapeutic benefit that could be obtained from inactivating the RNF degradation pathways.

Acknowledgments—We thank M. Benharouga, P. Fanen, A. Hinzpeter, A. Edelman, and F. Brouillard for advice and reagents on CFTR and E. Chevet for the α1-antitrypsin-expressing plasmids. We thank J. C. Aude and J. Y. Thuret for their help in phylogenetic analysis and modelization, respectively. We thank all members of the Toledano laboratory for fruitful discussions. We are very grateful to Ze'ev Ronai for help in setting up this project, by providing reagents, advice, and useful comments along the way.

APPENDIX

For fitting curves and modelization, the experimental data obtained from the CHX experiment were fitted to the exponential decay function in Equation 1,

$$m(t) = m_0 \cdot e^{-kt} \quad \text{(Eq. 1)}$$

where m_0 is the initial number of full-length proteins; k is the degradation rate, and $m(t)$ is the number of full-length proteins remaining at time t.

Fitting curves were obtained using the R software and produced Equations 2–4,

$$m_{vector}(t) = 100e^{-0.016t} \quad \text{(Eq. 2)}$$

and

$$m_{RNF185}(t) = 100e^{-0.023t}, \quad \text{(Eq. 3)}$$

identifying

$$k_{vector} = 0.0164 \text{ and } k_{RNF185} = 0.0234 \quad \text{(Eq. 4)}$$

The ^{35}S labeling experiment was modeled as follows. If one considers that S, the rate of synthesis (*i.e.* the number of full-length proteins synthesized by time unit), is constant over time, then we get Equation 5,

$$dm/dt = S - km \quad \text{(Eq. 5)}$$

where m is the number of full-length proteins; t is the time, and k is the degradation rate that is established by the CHX experiment.

It follows that Equation 6 is the result,

$$m(t) = ((S/k) \cdot e^{-kt}) + C, \quad \text{(Eq. 6)}$$

where C is a constant.

At $t = 0$, $m(0) = 0$, hence $C = -S/k$; therefore, Equation 7

$$m(t) = S/k \cdot (1 - e^{-kt}) \quad \text{(Eq. 7)}$$

is the function that predicts the accumulation of full-length protein over time. S can be decomposed as the rate of translation minus the rate of co-translational degradation. If one consider the ratio shown in Equation 8,

$$m_{RNF185}(t)/m_{vector}(t) = (S_{RNF185}/k_{RNF185} \cdot (1 - e^{-k_{RNF185} \cdot t})) / (S_{vector}/k_{vector} \cdot (1 - e^{-k_{vector} \cdot t})), \quad \text{(Eq. 8)}$$

and if co-translational degradation is absent, S only reflects the rate of translation, which appears similar in the control sample and upon overexpressing RNF185 and Equation 9.

$$S_{RNF185} = S_{vector}, \quad \text{(Eq. 9)}$$

Therefore, we achieve Equation 10,

$$m_{RNF185}(t)/m_{vector}(t) = k_{vector}/k_{RNF185} \cdot (1 - e^{-k_{RNF185}t})/(1 - e^{k_{vector}t}). \quad \text{(Eq. 10)}$$

Using $k_{vector} = 0.016$ and $k_{RNF185} = 0.023$ from the CHX experiment, it follows that at 20 min the expected ratio in the absence of co-translational degradation is Equation 11.

$$m_{RNF185}(t)/m_{vector}(t) = 0.937. \quad \text{(Eq. 11)}$$

which corresponds to a 6.3% decrease in ^{35}S-labeled CFTR in the presence of RNF185 compared with the control condition.

REFERENCES

1. Brodsky, J. L., and McCracken, A. A. (1999) ER protein quality control and proteasome-mediated protein degradation. *Semin. Cell Dev. Biol.* **10,** 507–513
2. Ellgaard, L., and Helenius, A. (2003) Quality control in the endoplasmic reticulum. *Nat. Rev. Mol. Cell Biol.* **4,** 181–191
3. Sitia, R., and Braakman, I. (2003) Quality control in the endoplasmic reticulum protein factory. *Nature* **426,** 891–894
4. Hebert, D. N., and Molinari, M. (2007) In and out of the ER: protein folding, quality control, degradation, and related human diseases. *Physiol. Rev.* **87,** 1377–1408
5. Vembar, S. S., and Brodsky, J. L. (2008) One step at a time: endoplasmic reticulum-associated degradation. *Nat. Rev. Mol. Cell Biol.* **9,** 944–957
6. Hershko, A., and Ciechanover, A. (1992) The ubiquitin system for protein degradation. *Annu. Rev. Biochem.* **61,** 761–807
7. Lenk, U., Yu, H., Walter, J., Gelman, M. S., Hartmann, E., Kopito, R. R., and Sommer, T. (2002) A role for mammalian Ubc6 homologues in ER-associated protein degradation. *J. Cell Sci.* **115,** 3007–3014
8. Tiwari, S., and Weissman, A. M. (2001) Endoplasmic reticulum (ER)-associated degradation of T cell receptor subunits. Involvement of ER-associated ubiquitin-conjugating enzymes (E2s). *J. Biol. Chem.* **276,** 16193–16200
9. Hirsch, C., Gauss, R., Horn, S. C., Neuber, O., and Sommer, T. (2009) The ubiquitylation machinery of the endoplasmic reticulum. *Nature* **458,** 453–460
10. Kostova, Z., Tsai, Y. C., and Weissman, A. M. (2007) Ubiquitin ligases,

critical mediators of endoplasmic reticulum-associated degradation. *Semin. Cell Dev. Biol.* **18,** 770–779
11. Bays, N. W., Gardner, R. G., Seelig, L. P., Joazeiro, C. A., and Hampton, R. Y. (2001) Hrd1p/Der3p is a membrane-anchored ubiquitin ligase required for ER-associated degradation. *Nat. Cell Biol.* **3,** 24–29
12. Bordallo, J., Plemper, R. K., Finger, A., and Wolf, D. H. (1998) Der3p/Hrd1p is required for endoplasmic reticulum-associated degradation of misfolded lumenal and integral membrane proteins. *Mol. Biol. Cell* **9,** 209–222
13. Gauss, R., Jarosch, E., Sommer, T., and Hirsch, C. (2006) A complex of Yos9p and the HRD ligase integrates endoplasmic reticulum quality control into the degradation machinery. *Nat. Cell Biol.* **8,** 849–854
14. Sato, S., Ward, C. L., and Kopito, R. R. (1998) Cotranslational ubiquitination of cystic fibrosis transmembrane conductance regulator *in vitro*. *J. Biol. Chem.* **273,** 7189–7192
15. Denic, V., Quan, E. M., and Weissman, J. S. (2006) A luminal surveillance complex that selects misfolded glycoproteins for ER-associated degradation. *Cell* **126,** 349–359
16. Carvalho, P., Goder, V., and Rapoport, T. A. (2006) Distinct ubiquitin-ligase complexes define convergent pathways for the degradation of ER proteins. *Cell* **126,** 361–373
17. Gauss, R., Sommer, T., and Jarosch, E. (2006) The Hrd1p ligase complex forms a linchpin between ER-lumenal substrate selection and Cdc48p recruitment. *EMBO J.* **25,** 1827–1835
18. Braun, S., Matuschewski, K., Rape, M., Thoms, S., and Jentsch, S. (2002) Role of the ubiquitin-selective CDC48(UFD1/NPL4)chaperone (segregase) in ERAD of OLE1 and other substrates. *EMBO J.* **21,** 615–621
19. Jarosch, E., Taxis, C., Volkwein, C., Bordallo, J., Finley, D., Wolf, D. H., and Sommer, T. (2002) Protein dislocation from the ER requires polyubiquitination and the AAA-ATPase Cdc48. *Nat. Cell Biol.* **4,** 134–139
20. Ye, Y., Meyer, H. H., and Rapoport, T. A. (2001) The AAA ATPase Cdc48/p97 and its partners transport proteins from the ER into the cytosol. *Nature* **414,** 652–656
21. Ye, Y., Shibata, Y., Kikkert, M., van Voorden, S., Wiertz, E., and Rapoport, T. A. (2005) Recruitment of the p97 ATPase and ubiquitin ligases to the site of retrotranslocation at the endoplasmic reticulum membrane. *Proc. Natl. Acad. Sci. U.S.A.* **102,** 14132–14138
22. Iida, Y., Fujimori, T., Okawa, K., Nagata, K., Wada, I., and Hosokawa, N. (2011) SEL1L protein critically determines the stability of the HRD1-SEL1L endoplasmic reticulum-associated degradation (ERAD) complex to optimize the degradation kinetics of ERAD substrates. *J. Biol. Chem.* **286,** 16929–16939
23. Lilley, B. N., and Ploegh, H. L. (2004) A membrane protein required for dislocation of misfolded proteins from the ER. *Nature* **429,** 834–840
24. Oda, Y., Okada, T., Yoshida, H., Kaufman, R. J., Nagata, K., and Mori, K. (2006) Derlin-2 and Derlin-3 are regulated by the mammalian unfolded protein response and are required for ER-associated degradation. *J. Cell Biol.* **172,** 383–393
25. Sun, F., Zhang, R., Gong, X., Geng, X., Drain, P. F., and Frizzell, R. A. (2006) Derlin-1 promotes the efficient degradation of the cystic fibrosis transmembrane conductance regulator (CFTR) and CFTR folding mutants. *J. Biol. Chem.* **281,** 36856–36863
26. Ye, Y., Shibata, Y., Yun, C., Ron, D., and Rapoport, T. A. (2004) A membrane protein complex mediates retro-translocation from the ER lumen into the cytosol. *Nature* **429,** 841–847
27. Younger, J. M., Chen, L., Ren, H. Y., Rosser, M. F., Turnbull, E. L., Fan, C. Y., Patterson, C., and Cyr, D. M. (2006) Sequential quality-control checkpoints triage misfolded cystic fibrosis transmembrane conductance regulator. *Cell* **126,** 571–582
28. Greenblatt, E. J., Olzmann, J. A., and Kopito, R. R. (2011) Derlin-1 is a rhomboid pseudoprotease required for the dislocation of mutant α-1 antitrypsin from the endoplasmic reticulum. *Nat. Struct. Mol. Biol.* **18,** 1147–1152
29. Carroll, S. M., and Hampton, R. Y. (2010) Usa1p is required for optimal function and regulation of the Hrd1p endoplasmic reticulum-associated degradation ubiquitin ligase. *J. Biol. Chem.* **285,** 5146–5156
30. Horn, S. C., Hanna, J., Hirsch, C., Volkwein, C., Schütz, A., Heinemann, U., Sommer, T., and Jarosch, E. (2009) Usa1 functions as a scaffold of the HRD-ubiquitin ligase. *Mol. Cell* **36,** 782–793
31. Kny, M., Standera, S., Hartmann-Petersen, R., Kloetzel, P. M., and Seeger, M. (2011) Herp regulates Hrd1-mediated ubiquitylation in a ubiquitin-like domain-dependent manner. *J. Biol. Chem.* **286,** 5151–5156
32. Huyer, G., Piluek, W. F., Fansler, Z., Kreft, S. G., Hochstrasser, M., Brodsky, J. L., and Michaelis, S. (2004) Distinct machinery is required in *Saccharomyces cerevisiae* for the endoplasmic reticulum-associated degradation of a multispanning membrane protein and a soluble luminal protein. *J. Biol. Chem.* **279,** 38369–38378
33. Nakatsukasa, K., and Brodsky, J. L. (2008) The recognition and retrotranslocation of misfolded proteins from the endoplasmic reticulum. *Traffic* **9,** 861–870
34. Ravid, T., and Hochstrasser, M. (2008) Diversity of degradation signals in the ubiquitin-proteasome system. *Nat. Rev. Mol. Cell Biol.* **9,** 679–690
35. Bernardi, K. M., Williams, J. M., Kikkert, M., van Voorden, S., Wiertz, E. J., Ye, Y., and Tsai, B. (2010) The E3 ubiquitin ligases Hrd1 and gp78 bind to and promote cholera toxin retro-translocation. *Mol. Biol. Cell* **21,** 140–151
36. Bernasconi, R., Galli, C., Calanca, V., Nakajima, T., and Molinari, M. (2010) Stringent requirement for HRD1, SEL1L, and OS-9/XTP3-B for disposal of ERAD-LS substrates. *J. Cell Biol.* **188,** 223–235
37. Chen, B., Mariano, J., Tsai, Y. C., Chan, A. H., Cohen, M., and Weissman, A. M. (2006) The activity of a human endoplasmic reticulum-associated degradation E3, gp78, requires its Cue domain, RING finger, and an E2-binding site. *Proc. Natl. Acad. Sci. U.S.A.* **103,** 341–346
38. Christianson, J. C., Olzmann, J. A., Shaler, T. A., Sowa, M. E., Bennett, E. J., Richter, C. M., Tyler, R. E., Greenblatt, E. J., Harper, J. W., and Kopito, R. R. (2012) Defining human ERAD networks through an integrative mapping strategy. *Nat. Cell Biol.* **14,** 93–105
39. Kikkert, M., Doolman, R., Dai, M., Avner, R., Hassink, G., van Voorden, S., Thanedar, S., Roitelman, J., Chau, V., and Wiertz, E. (2004) Human HRD1 is an E3 ubiquitin ligase involved in degradation of proteins from the endoplasmic reticulum. *J. Biol. Chem.* **279,** 3525–3534
40. Meacham, G. C., Patterson, C., Zhang, W., Younger, J. M., and Cyr, D. M. (2001) The Hsc70 co-chaperone CHIP targets immature CFTR for proteasomal degradation. *Nat. Cell Biol.* **3,** 100–105
41. Rosser, M. F., Grove, D. E., Chen, L., and Cyr, D. M. (2008) Assembly and misassembly of cystic fibrosis transmembrane conductance regulator: folding defects caused by deletion of F508 occur before and after the calnexin-dependent association of membrane spanning domain (MSD) 1 and MSD2. *Mol. Biol. Cell* **19,** 4570–4579
42. Younger, J. M., Ren, H. Y., Chen, L., Fan, C. Y., Fields, A., Patterson, C., and Cyr, D. M. (2004) A foldable CFTRΔF508 biogenic intermediate accumulates upon inhibition of the Hsc70-CHIP E3 ubiquitin ligase. *J. Cell Biol.* **167,** 1075–1085
43. Grove, D. E., Fan, C. Y., Ren, H. Y., and Cyr, D. M. (2011) The endoplasmic reticulum-associated Hsp40 DNAJB12 and Hsc70 cooperate to facilitate RMA1 E3-dependent degradation of nascent CFTRΔF508. *Mol. Biol. Cell* **22,** 301–314
44. Wang, B., Heath-Engel, H., Zhang, D., Nguyen, N., Thomas, D. Y., Hanrahan, J. W., and Shore, G. C. (2008) BAP31 interacts with Sec61 translocons and promotes retrotranslocation of CFTRΔF508 via the derlin-1 complex. *Cell* **133,** 1080–1092
45. Morito, D., Hirao, K., Oda, Y., Hosokawa, N., Tokunaga, F., Cyr, D. M., Tanaka, K., Iwai, K., and Nagata, K. (2008) Gp78 cooperates with RMA1 in endoplasmic reticulum-associated degradation of CFTRΔF508. *Mol. Biol. Cell* **19,** 1328–1336
46. Fang, S., Ferrone, M., Yang, C., Jensen, J. P., Tiwari, S., and Weissman, A. M. (2001) The tumor autocrine motility factor receptor, gp78, is a ubiquitin protein ligase implicated in degradation from the endoplasmic reticulum. *Proc. Natl. Acad. Sci. U.S.A.* **98,** 14422–14427
47. DeLaBarre, B., Christianson, J. C., Kopito, R. R., and Brunger, A. T. (2006) Central pore residues mediate the p97/VCP activity required for ERAD. *Mol. Cell* **22,** 451–462
48. Delaunay, A., Bromberg, K. D., Hayashi, Y., Mirabella, M., Burch, D., Kirkwood, B., Serra, C., Malicdan, M. C., Mizisin, A. P., Morosetti, R., Broccolini, A., Guo, L. T., Jones, S. N., Lira, S. A., Puri, P. L., Shelton, G. D., and Ronai, Z. (2008) The ER-bound RING finger protein 5 (RNF5/RMA1)

causes degenerative myopathy in transgenic mice and is deregulated in inclusion body myositis. *PLoS One* **3,** e1609
49. Fanen, P., Clain, J., Labarthe, R., Hulin, P., Girodon, E., Pagesy, P., Goossens, M., and Edelman, A. (1999) Structure-function analysis of a double-mutant cystic fibrosis transmembrane conductance regulator protein occurring in disorders related to cystic fibrosis. *FEBS Lett.* **452,** 371–374
50. Tang, F., Wang, B., Li, N., Wu, Y., Jia, J., Suo, T., Chen, Q., Liu, Y. J., and Tang, J. (2011) RNF185, a novel mitochondrial ubiquitin E3 ligase, regulates autophagy through interaction with BNIP1. *PLoS One* **6,** e24367
51. Pearce, M. M., Wang, Y., Kelley, G. G., and Wojcikiewicz, R. J. (2007) SPFH2 mediates the endoplasmic reticulum-associated degradation of inositol 1,4,5-trisphosphate receptors and other substrates in mammalian cells. *J. Biol. Chem.* **282,** 20104–20115
52. Travers, K. J., Patil, C. K., Wodicka, L., Lockhart, D. J., Weissman, J. S., and Walter, P. (2000) Functional and genomic analyses reveal an essential coordination between the unfolded protein response and ER-associated degradation. *Cell* **101,** 249–258
53. Jensen, T. J., Loo, M. A., Pind, S., Williams, D. B., Goldberg, A. L., and Riordan, J. R. (1995) Multiple proteolytic systems, including the proteasome, contribute to CFTR processing. *Cell* **83,** 129–135
54. Ward, C. L., and Kopito, R. R. (1994) Intracellular turnover of cystic fibrosis transmembrane conductance regulator. Inefficient processing and rapid degradation of wild-type and mutant proteins. *J. Biol. Chem.* **269,** 25710–25718
55. Ward, C. L., Omura, S., and Kopito, R. R. (1995) Degradation of CFTR by the ubiquitin-proteasome pathway. *Cell* **83,** 121–127
56. Huppa, J. B., and Ploegh, H. L. (1997) The α chain of the T cell antigen receptor is degraded in the cytosol. *Immunity* **7,** 113–122
57. Yang, M., Omura, S., Bonifacino, J. S., and Weissman, A. M. (1998) Novel aspects of degradation of T cell receptor subunits from the endoplasmic reticulum (ER) in T cells: importance of oligosaccharide processing, ubiquitination, and proteasome-dependent removal from ER membranes. *J. Exp. Med.* **187,** 835–846
58. Yu, H., Kaung, G., Kobayashi, S., and Kopito, R. R. (1997) Cytosolic degradation of T-cell receptor α chains by the proteasome. *J. Biol. Chem.* **272,** 20800–20804
59. Yu, H., and Kopito, R. R. (1999) The role of multiubiquitination in dislocation and degradation of the α subunit of the T cell antigen receptor. *J. Biol. Chem.* **274,** 36852–36858
60. Kamimoto, T., Shoji, S., Hidvegi, T., Mizushima, N., Umebayashi, K., Perlmutter, D. H., and Yoshimori, T. (2006) Intracellular inclusions containing mutant α1-antitrypsin Z are propagated in the absence of autophagic activity. *J. Biol. Chem.* **281,** 4467–4476
61. Liu, Y., Choudhury, P., Cabral, C. M., and Sifers, R. N. (1997) Intracellular disposal of incompletely folded human α1-antitrypsin involves release from calnexin and post-translational trimming of asparagine-linked oligosaccharides. *J. Biol. Chem.* **272,** 7946–7951
62. Qu, D., Teckman, J. H., Omura, S., and Perlmutter, D. H. (1996) Degradation of a mutant secretory protein, α1-antitrypsin Z, in the endoplasmic reticulum requires proteasome activity. *J. Biol. Chem.* **271,** 22791–22795
63. Teckman, J. H., Gilmore, R., and Perlmutter, D. H. (2000) Role of ubiquitin in proteasomal degradation of mutant α(1)-antitrypsin Z in the endoplasmic reticulum. *Am. J. Physiol. Gastrointest. Liver Physiol.* **278,** G39–G48
64. Markson, G., Kiel, C., Hyde, R., Brown, S., Charalabous, P., Bremm, A., Semple, J., Woodsmith, J., Duley, S., Salehi-Ashtiani, K., Vidal, M., Komander, D., Serrano, L., Lehner, P., and Sanderson, C. M. (2009) Analysis of the human E2 ubiquitin conjugating enzyme protein interaction network. *Genome Res.* **19,** 1905–1911
65. Lukacs, G. L., and Verkman, A. S. (2012) CFTR: folding, misfolding, and correcting the ΔF508 conformational defect. *Trends Mol. Med.* **18,** 81–91
66. Tcherpakov, M., Delaunay, A., Toth, J., Kadoya, T., Petroski, M. D., and Ronai, Z. A. (2009) Regulation of endoplasmic reticulum-associated degradation by RNF5-dependent ubiquitination of JNK-associated membrane protein (JAMP). *J. Biol. Chem.* **284,** 12099–12109
67. Zhong, B., Zhang, L., Lei, C., Li, Y., Mao, A. P., Yang, Y., Wang, Y. Y., Zhang, X. L., and Shu, H. B. (2009) The ubiquitin ligase RNF5 regulates antiviral responses by mediating degradation of the adaptor protein MITA. *Immunity* **30,** 397–407
68. Zhong, B., Zhang, Y., Tan, B., Liu, T. T., Wang, Y. Y., and Shu, H. B. (2010) The E3 ubiquitin ligase RNF5 targets virus-induced signaling adaptor for ubiquitination and degradation. *J. Immunol.* **184,** 6249–6255
69. Zhang, Q., Wu, J., Wu, R., Ma, J., Du, G., Jiao, R., Tian, Y., Zheng, Z., and Yuan, Z. (2012) DJ-1 promotes the proteasomal degradation of Fis1: implications of DJ-1 in neuronal protection. *Biochem. J.* **447,** 261–269
70. Kuang, E., Okumura, C. Y., Sheffy-Levin, S., Varsano, T., Shu, V. C., Qi, J., Niesman, I. R., Yang, H. J., López-Otín, C., Yang, W. Y., Reed, J. C., Broday, L., Nizet, V., and Ronai, Z. A. (2012) Regulation of ATG4B stability by RNF5 limits basal levels of autophagy and influences susceptibility to bacterial infection. *PLoS Genet.* **8,** e1003007
71. Iioka, H., Iemura, S., Natsume, T., and Kinoshita, N. (2007) Wnt signalling regulates paxillin ubiquitination essential for mesodermal cell motility. *Nat. Cell Biol.* **9,** 813–821